Poisson channel with binary Markov input and average sojourn time constraint

Mark Sinzger, Maximilian Gehri, Heinz Koeppl
Dept. of Electrical Engineering, Centre for Synthetic Biology, Technische Universität Darmstadt
Darmstadt, Germany
Email: {mark.sinzger,maximilian.gehri,heinz.koeppl}@bcs.tu-darmstadt.de

arXiv:2101.01607v1 [q-bio.MN] 5 Jan 2021

***Abstract*—A minimal model for gene expression, consisting of a switchable promoter together with the resulting messenger RNA, is equivalent to a Poisson channel with a binary Markovian input process. Determining its capacity is an optimization problem with respect to two parameters: the average sojourn times of the promoter's active (ON) and inactive (OFF) state. An expression for the mutual information is found by solving the associated filtering problem analytically on the level of distributions. For fixed peak power, three bandwidth-like constraints are imposed by lower-bounding (i) the average sojourn times (ii) the autocorrelation time and (iii) the average time until a transition. OFF-favoring optima are found for all three constraints, as commonly encountered for the Poisson channel. In addition, constraint (i) exhibits a region that favors the ON state, and (iii) shows ON-favoring local optima.**

***Index Terms*—Poisson channel, gene expression, binary Markov, average sojourn time, filtering, bandwidth constraint**

I. Introduction

There is mounting evidence that the information encoded in the temporal concentration profiles of biomolecules plays a key role in cellular sensing and decision making [1], [2] and helps to overcome biochemical noise [3]. The computation of mutual information (MI) between time-varying, biomolecular signals is complex, and analytical solutions so far relied on Gaussian [4] or steady-state approximations [5]. Other papers have focused on single time-point transmission, e.g., [6], [7]. Works, that account for the discrete nature of chemical reactions, commonly assume diffusion approximations as inputs [8], [9] or are based on stochastic simulation [**?**], [10], [11]. Restrictions to sub-classes of discrete-state input processes permit analytical bounds on the capacity [12], often challenging diffusion based results [13].

This paper analyzes the minimal gene expression model with a two-state promoter (see e.g. [14] and Fig. 2a in [15]) as an analytically tractable example. Switching stochastically between activated state x_1 and inactivated state x_2, the promoter is modeled by a stationary random telegraph process $X(t)$, i.e., a binary, time-homogeneous, stationary Markov process (BMP). Its state linearly modulates the synthesis rate of messenger RNA molecules $Y(t)$. The decay of mRNA molecules can be ignored from an information theoretic point of view, because birth events are uniquely identified from birth-death trajectories [10]. The joint distribution of (X, Y), that factorizes in the conditional $Y|X$ and the input path distribution μ_X, is equivalent to the Poisson channel, whose class of input processes $X(t)$ is restricted to BMPs. We distinguish between channels with leakage ($x_1 > 0$) and without leakage ($x_1 = 0$), see Fig. 1a. By $X_{[0,T]}$ we denote the trajectory $X(t)_{0\le t\le T}$ of the time-varying input signal with transmission duration T. The sojourn times σ_1 in x_1 and σ_2 in x_2 are exponentially distributed with parameters c_1 and c_2 such that $\mathbb{E}[\sigma_1] = c_1^{-1}$ and $\mathbb{E}[\sigma_2] = c_2^{-1}$. The channel output $Y(t)$ fires at rate $c_3X(t)$, where c_3 is the channel gain that dictates the time scale of $Y(t)$. We denote the jump times of Y as t_i with $0 < t_1 < \cdots < T$.

The Poisson channel was introduced as a model for direct-detection optical communication systems [16]. Classically, peak and average power are constrained. Then among general inputs the class of BMPs achieves capacity, however at the cost of infinite switching rates c_1, c_2 [17], [18]. This physical implausibility motivates bandwidth-like constraints [19], [20]. By restricting general signals to binary inputs with lower-bounded sojourn times, [21] reported a transition from asymmetric to symmetric allocation for the capacity-achieving input, as the lower bound increases.

A. Problem statement and outline

We consider the Poisson channel with BMPs as input class and investigate the following bandwidth-like constraints:

- (C1) $0 < c_1 \le r_1, 0 < c_2 \le r_2$, i.e., lower-bounding the average sojourn times by $\mathbb{E}[\sigma_1] \ge r_1^{-1}, \mathbb{E}[\sigma_2] \ge r_2^{-1}$. A special case is the homogeneous constraint $\max\{c_1, c_2\} \le r_0$, in analogy to [21].
- (C2) $0 < c_1 + c_2 \le r_0$. Since $\mathbb{C}\mathrm{ov}[X(t), X(t+s)] \propto \exp(-(c_1 + c_2)s)$, this bounds the autocorrelation time of $X(t)$ from below.
- (C3) $\mathbb{E}[\mathbb{E}[\sigma_{X(t)}|X(t)]] = c_1^{-1} + c_2^{-1} - 2/(c_1 + c_2) \ge r_0^{-1}$, which lower-bounds the average sojourn time, similarly to (C1), but regardless of the transition type.

As the biophysical interpretation and value of the rates c_1, c_2 strongly depends on the context of the promoter model [15], [22]–[24] we list some generic motivations. The timescales

The work was supported by the European Research Council (ERC) within the Consolidator Grant CONSYN (grant agreement no. 773196).

This article was accepted for publication by IEEE, ISIT 2020.
doi: 10.1109/ISIT44484.2020.9174360 ©2020 IEEE

of the rates may be determined by binding affinity to the promoter, temperature, diffusion [25], [26], and availability of activating and deactivating constituents, such as transcription factors, polymerases, other enzymes, or ATP. Highly autocorrelated dynamics may be caused by upstream regulation or feedback of downstream elements in a reaction network [8], [27].

We consider the path-wise MI $\mathbb{I}(X_{[0,T]}, Y_{[0,T]})$ [28] and the information rate, defined as

$$\bar{\mathbb{I}}(X,Y) := \lim_{T\to\infty} \frac{1}{T}\mathbb{I}(X_{[0,T]}, Y_{[0,T]}).$$

Optimizing (i) the MI and (ii) the information rate with respect to all admissible input path distributions μ_X yields (i) the capacity C_T and (ii) the information rate capacity C. For fixed OFF and ON states x_1, x_2, the distribution μ_X is parametrized solely by the system parameters $c_1, c_2 \geq 0$. Fixing c_3, the respective capacity-achieving path distributions are characterized by the following constrained optimization problems

$$\text{(i)} \ \max_{c_1,c_2} \frac{1}{T}\mathbb{I}(X_{[0,T]}, Y_{[0,T]}), \quad \text{(ii)} \ \max_{c_1,c_2} \bar{\mathbb{I}}(X,Y)$$

subject to one of the constraints (C1) to (C3).

The remainder of the work is organized as follows. Exploiting the link between MI and filtering, section II addresses the associated filtering problem [29] analytically on the level of distributions. We recognize the conditional mean as a piecewise deterministic Markov process [30], and solve the partial differential equation (PDE) given by the hybrid generator [31]. In section III we express the MI and information rate as nonelementary Riemann integrals related to hypergeometric series. This permits further analysis of the constraints (C1) to (C3). Capacity-achieving input was reported so far as asymmetric, favoring the OFF state [17], [18]. In contrast, we find that constraint (C1) either enforces a symmetric allocation of ON and OFF state at optimality for certain r_1, r_2 or favors the ON state. ON-favoring local optima are implied by (C3).

B. Previous Work

The following expression due to [28] links the path-wise MI with the filtering problem of observing the input X indirectly via the Poisson channel output Y. Accordingly,

$$\mathbb{I}(X_{[0,T]}, Y_{[0,T]}) = \int_0^T \mathbb{E}[\phi(c_3 X(t))] - \mathbb{E}[\phi(c_3 Z(t))] \, \mathrm{d}t, \quad (1)$$

where $\phi(z) = z\ln(z)$ and the first conditional moment $Z(t) = \mathbb{E}[X(t) \mid Y_{[0,t]}]$ is the optimal causal estimator of the input under a quadratic criterion.

Applying Jensen's inequality to the second integrand term of (1) and using the identity $\phi(cz) = c\phi(z) + z\phi(c)$ as well as the stationarity of BMPs, the MI is bounded by

$$\begin{aligned}\frac{\mathbb{I}(X_{[0,T]}, Y_{[0,T]})}{c_3 T} &\leq \frac{c_2\phi(x_1) + c_1\phi(x_2)}{c_1+c_2} - \phi\left(x_1 + \frac{c_1\Delta x}{c_1+c_2}\right) \\ &=: J(x_1, x_2, c_1/(c_1+c_2)),\end{aligned}$$

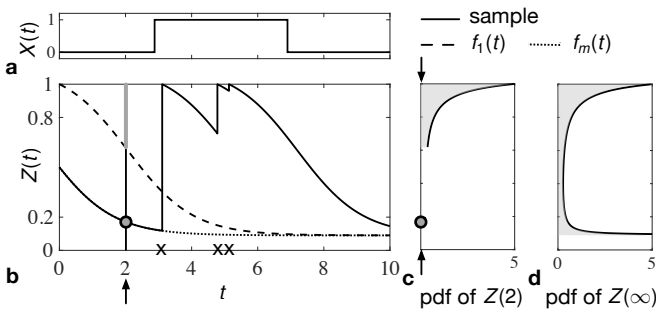


Fig. 1. Dynamics of the causal estimator $Z(t)$ for $c_1 = c_2 = 0.1, c_3 = 1, x_1 = 0, x_2 = 1$. **a** Sample trajectory of the binary signal input $X(t)$. **b** The solid line is a sample trajectory of $Z(t)$. Crosses indicate the jump times t_1, t_2, t_3 of Y. The dotted line $f_m(t)$ is the common trajectory of $Z(t)$ prior to the first jump. The dashed line $f_1(t)$ separates the (t,z)-plane. Prior to the first jump the trajectories evolve below, afterwards they evolve above. **c** The probability distribution of the causal estimator at time $t = 2$ is composed of a Dirac measure with weight $\kappa(2)$ at $f_m(2)$ and a density supported on $(f_1(2), 1]$. **d** Probability density of the asymptotic causal estimator.

where $\Delta x := x_2 - x_1$ is the dynamic range. Optimizing over the average power constraint $0 < c_1/(c_1+c_2) \leq p_0$ implies

$$C \leq c_3 J(x_1, x_2, \min\{p_0, \bar{p}\}), \quad (2)$$

where C can be replaced by C_T and

$$\bar{p} = \left\{\exp\left(\frac{\phi(x_2) - \phi(x_1)}{\Delta x} - 1\right) - x_1\right\} / \Delta x.$$

Kabanov and Davis showed that for $c_1, c_2 \to \infty$ the bound (2) is indeed achieved with the respective asymptotic ratio $c_1/(c_1+c_2) = \min\{p_0, \bar{p}\}$ [17], [18]. The case $x_1 = 0, x_2 = 1$ (no leakage) with $p_0 \geq 1/e$ reduces to $C = C_T = c_3/e$ with $c_1/(c_1+c_2) = 1/e$.

We contribute by analyzing how the capacity-achieving BMP input behaves for finite c_1, c_2, reflected in the bandwidth-like constraints (C1) to (C3). For the process class of BMPs, $Z(t)$ in (1) evolves according to the ODE with stochastic jumps [29]

$$\begin{aligned}\mathrm{d}Z(t) = &[c_1 \cdot \Delta x - (c_1 + c_2 + c_3 \cdot \Delta x)(Z(t) - x_1) \\ &+ c_3 (Z(t) - x_1)^2] \ \mathrm{d}t + g(Z(t)) \ \mathrm{d}Y(t),\end{aligned} \quad (3)$$

where $\mathrm{d}Y(t) = 1$ for jump times $t = t_i$, vanishing otherwise; and $g(Z(t_i)) = \frac{(Z(t_i)-x_1)(x_2 - Z(t_i))}{Z(t_i)}$ is the jump height $\mathrm{d}Z(t_i) = Z(t_i+) - Z(t_i-)$ at jump times of Y. Fig. 1b shows a sample trajectory for $x_1 = 0, x_2 = 1$.

II. The solution of the filtering problem

In the following, we solve for the distribution of $Z(t)$, provided that leakage is absent ($x_1 = 0$) and the dynamic range is normalized ($x_2 = 1$). This self-noise limited case allows for an analytic expression of the MI in III-A.

A. The probability evolution equation

In absence of leakage the stochastic reset condition in (3) simplifies, because $Y(t)$ increases solely if $X(t)$ is in the ON state. Hence, $Z(t)$ is reset to $x_2 = 1$ upon jumps

of Y. The joint process $\{Z(t), Y(t)\}_t$ is then a piece-wise deterministic Markov process [30] that jumps stochastically from state $\{Z(t_i-), Y(t_i-)\}$ to state $\{Z(t_i+), Y(t_i+)\} = (1, Y(t_i-) + 1)$. Hence, jump times t_i of Y and of Z are identical, and jumps occur with propensity $c_3 Z(t)$ [29]. Since the propensity depends only on the first component, the projection onto $Z(t)$ is a piece-wise deterministic Markov process itself. Its probability evolution equation is given by a hybrid generator, composed of the drift (Liouville) and the jump (Poisson) part [31]:

$$\frac{\partial}{\partial t}p(t,z) = -\frac{\partial}{\partial z}\{A(z)p(t,z)\} - c_3 z p(t,z),\ \omega < z < 1, \quad (4)$$

where $A(z) := c_3(c_1\Delta x/c_3 - \gamma z + z^2)$ with $\gamma := (c_1 + c_2 + \Delta x c_3)/c_3$ is the drift dynamics, i.e., the ODE part of (3) with stable equilibrium $\omega := \frac{\gamma-\rho}{2}$, where $\rho := \sqrt{\gamma^2 - 4c_1\Delta x/c_3}$. The reason why (4) is lacking an inflow of probability due to jumps is because all inflow enters at $z = 1$. This is reflected in the proof of the subsequent theorem II.1. Although expression (1) has been used and extended [32] in multiple ways to address the capacity problem, to the best of our knowledge, the method introduced here is new to the field.

B. Transient and asymptotic distribution

Aiming for the distribution of $Z(t)$, we envision the stochastic ensemble of trajectories. All trajectories are initiated in the stationary mean $m := c_1/(c_1 + c_2)$, because $Z(0) = \mathbb{E}[X(0)]$. They slide down according to the function

$$f_\iota(t) = \omega + \frac{\rho(\iota - \omega)}{\iota - \omega + e^{\rho c_3 t}(\rho + \omega - \iota)}$$

with $\iota = m$ (see Fig. 1b), which solves the Riccati equation $\frac{\mathrm{d}}{\mathrm{d}t}Z(t) = A(Z(t))$. The solution curve $f_1(t)$ with initial value $z = 1$ at $t = 0$ separates the (t, z)-plane into two regions summarized in the equivalence that involves the first jump time t_1 of Z:

$$t < t_1 \Leftrightarrow Z(t) \le f_1(t) \Leftrightarrow Z(t) = f_m(t). \quad (5)$$

Fig. 1c visualizes the ensemble of trajectories stopped at a fixed t, while Fig. 1d visualizes the asymptotic probability distribution. The following theorem fully describes the distribution of $Z(t)$ at any time point t. Besides preparing the main result theorem III.1, it can be interesting in its own right in the related fields of filtering and control theory.

Theorem II.1. *The probability measure $\mu_t \colon \mathcal{B}(\omega, 1] \to [0, 1], \mu_t(B) = \mathbb{P}[Z(t) \in B]$, defined for Borel sets $B \subseteq (\omega, 1]$, is a hybrid measure*

$$\mu_t(B) = \kappa(t)\delta_{f_m(t)}(B) + \nu_t(B), \quad (6)$$

composed of a Dirac measure $\delta_a(B) = \mathbb{1}_B(a), a \in \mathbb{R}$ at $f_m(t)$ with weight

$$\kappa(t) = e^{-\omega c_3 t} \cdot \left(1 - \rho^{-1}(m - \omega)(1 - e^{-\rho c_3 t})\right)$$

and an absolutely continuous measure $\nu_t(\mathrm{d}z) = \pi(z)\mathrm{d}z$ supported on $(f_1(t), 1]$ with time-independent density

$$\pi(z) = \alpha(z - \omega)^{\beta - \frac{3}{2}}(\omega + \rho - z)^{-(\beta + \frac{3}{2})}, \quad (7)$$

where

$$\alpha := (1 - \omega)^{\frac{3}{2} - \beta}(\omega + \rho - 1)^{\beta + \frac{3}{2}} \cdot \frac{c_3 m}{c_2}, \quad \beta := \frac{\gamma}{2\rho}.$$

Proof. We use (5) and compute

$$\begin{aligned}\mathbb{P}[Z(t) \in B] &= \mathbb{P}[Z(t) \in B, t_1 > t] + \mathbb{P}[Z(t) \in B, t_1 \le t] \\ &= \mathbb{P}[t_1 > t]\delta_{f_m(t)}(B) + \mathbb{P}[Z(t) \in B \cap (f_1(t), 1]]\end{aligned}$$

having the form (6). First,

$$\mathbb{P}[t_1 > t] = \exp\left(-\int_0^t f_m(s)\ \mathrm{d}s\right) = \kappa(t).$$

Second, by the equivalence

$$Z(t) \in B \cap (f_1(t), 1] \Leftrightarrow t - \sup\{t_i \mid t_i \le t\} \in f_1^{-1}(B), t_1 \le t$$

the absolutely continuity of the t_i implies that $\nu_t(B) = \mathbb{P}[Z(t) \in B \cap (f_1(t), 1]]$ is an absolute continuous measure, i.e., $\nu_t(\mathrm{d}z) = p(t, z)\mathrm{d}z$ with some density $p(t, z)$ supported on $(f_1(t), 1]$. Its solution is obtained by the method of characteristics [33], initiated at the boundary condition $p_1(t) := p(t, 1)$ and propagated through the rewritten linear PDE (4)

$$\frac{\partial}{\partial t}p(t,z) + A(z)\frac{\partial}{\partial z}p(t,z) = p(t,z)\left\{-c_3 z - \frac{\mathrm{d}}{\mathrm{d}z}A(z)\right\}.$$

It remains to evaluate $p_1(t)$. We compute

$$\begin{aligned}\mathbb{E}[c_3 X(t)] &= \mathbb{E}\left[\lim_{h\to 0}\frac{\mathbb{P}[Y(t+h) - Y(t) = 1 \mid X_{[0,t]}]}{h}\right] \\ &= \lim_{h\to 0}\frac{\mathbb{P}[Y(t+h) - Y(t) = 1]}{h} \\ &= \lim_{h\to 0}\frac{\mathbb{P}[Z(t+h) \in (f_1(h), 1]]}{h} \\ &= -f_1'(t)p(t,1) = -A(1)p_1(t) = c_2 p_1(t).\end{aligned}$$

The absolute continuity of ν_t was used in the fourth equality. Stationarity of X implies that $p_1(t) \equiv c_3 m/c_2$ independent of t. Plugging this in, $p(t, z) = \pi(z)\mathbb{1}_{(f_1(t),1]}(z)$ is obtained. □

Theorem II.2. *The asymptotic distribution is absolutely continuous, supported on $(\omega, 1]$ with density $\pi(z)$ as in (7).*

Proof. Since $Z(t)$ is an ergodic Markov process, the asymptotic equals the stationary distribution. The distribution $\pi(z)$ satisfies the stationarity condition obtained from (4) by equating the right side to zero. □

III. The information surface

We consider the Poisson channel without leakage, unless mentioned otherwise.

A. Analytic expression

The results of the previous section allow us to state the main result of this paper.

Theorem III.1. *Let $x_1 = 0, x_2 = 1$, then*

$$\frac{1}{T}\mathbb{I}(X_{[0,T]}, Y_{[0,T]}) = -\frac{c_3}{T}\int_0^T \phi(f_m(t))\kappa(t)\ \mathrm{d}t - c_3\int_\omega^1 \phi(z)\pi(z)(1 - f_1^{-1}(z)/T)\ \mathrm{d}z,$$

$$\bar{\mathbb{I}}(X, Y) = -c_3\int_\omega^1 \phi(z)\pi(z)\ \mathrm{d}z.$$

Proof. Using theorems II.1,II.2, the identity $\phi(cz) = c\phi(z) + z\phi(c)$, and Fubini, evaluate (1). □

We use a linear transformation of the integration variable $z \to (1-z)(1-\omega)^{-1}$ and the series expansion of the logarithm as well as $z \mapsto (\rho+\omega-z)^{-\beta-3/2}$. Then by uniform convergence of the integrand, we may express

$$\bar{\mathbb{I}}(X, Y) = \sum_{i,j=0}^{\infty} A_{ij}\left(\frac{1-\omega}{\rho}\right)^j (1-\omega)^i, \tag{8}$$

as an absolutely convergent series with coefficients

$$A_{ij} = \frac{c_3\alpha\rho^{-\beta-\frac{3}{2}}(1-\omega)^{\beta+\frac{1}{2}}}{\Gamma(\beta+\frac{3}{2})} \times \frac{i!\Gamma(\beta+\frac{3}{2}+j)\Gamma(\beta-\frac{1}{2}+j)(\beta-\frac{1}{2}+j+\omega(i+2))}{j!\Gamma(\beta+\frac{5}{2}+i+j)},$$

establishing a link with Appell's hypergeometric F_3 series [34]. Using (8), it can be verified that for $c_1, c_2 \to \infty$ with asymptotic ratio $c_1/(c_1+c_2) \to p_0$, it holds that $\beta \to 1/2, \omega \to p_0$ and $(1-\omega)/\rho \to 0$. Hence $\bar{\mathbb{I}}(X, Y) \to c_3 J(0, 1, p_0)$, in accordance with paragraph I-B. Expanding $f_1^{-1}(z)$, the MI $\mathbb{I}(X_{[0,T]}, Y_{[0,T]})$ is given in terms of Srivastava's triple hypergeometric series [35] by analogous proceeding, implying

$$\frac{1}{T}\mathbb{I}(X_{[0,T]}, Y_{[0,T]}) \to c_3 J(0, 1, p_0)$$

for $c_1, c_2 \to \infty$ with asymptotic ratio $c_1/(c_1+c_2) \to p_0$.

The above linear transformation and subsequent differentiation under the integral sign or, alternatively, summand-wise differentiation of (8) make (higher-order) partial derivatives with respect to c_1, c_2 accessible for the phase plane analysis.

We introduce the relative rates $\tilde{c}_1 = c_1/c_3$ and $\tilde{c}_2 = c_2/c_3$. The parameters γ, ω, ρ and hence the stationary density $\pi(z)$ only depend on $\tilde{c}_1$ and $\tilde{c}_2$, and c_3 scales the time. The linear time scaling $\tilde{t} = c_3 t, \tilde{T} = c_3 T$ allows us to write the MI as

$$\frac{1}{T}\mathbb{I}(X_{[0,T]}, Y_{[0,T]}) = c_3 \cdot \frac{1}{\tilde{T}}\mathbb{I}(\tilde{X}_{[0,\tilde{T}]}, \tilde{Y}_{[0,\tilde{T}]}),$$

where $\tilde{X}(t)$ and $\tilde{Y}(t)$ are input and output of the correspondent channel with relative rates $\tilde{c}_1, \tilde{c}_2$ and normalized $\tilde{c}_3 = 1$. For convenience we drop the tilde in the following and assume a normalized time scale $c_3 = 1$ for the channel.

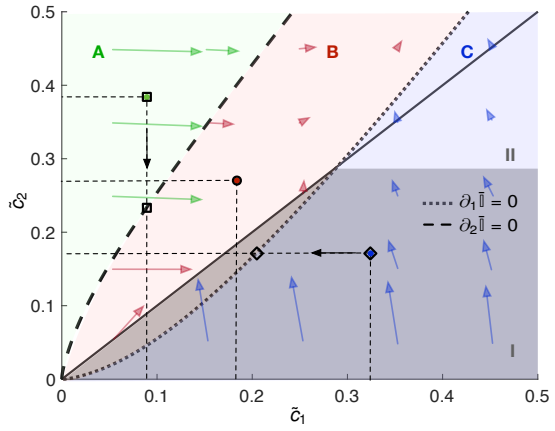


Fig. 2. Phase plane analysis of (C1) for $x_1 = 0, x_2 = 1$. Nullclines $\partial_1\bar{\mathbb{I}} = 0$ and $\partial_2\bar{\mathbb{I}} = 0$ were evaluated, using the first 100×100 summands of the F_3 series in (8) and deriving summand-wise. Colored arrows indicate the gradient of the information rate, calculated alike. Optimization domains are rectangular. Depending on the location of the domain's upper right corner (r_1, r_2), the optimum is assumed on the nullclines $\partial_1\bar{\mathbb{I}} = 0$ [(r_1, r_2) in C] and $\partial_2\bar{\mathbb{I}} = 0$ [(r_1, r_2) in A], respectively, or in the interior of region B [(r_1, r_2) in B]. Regions I and II contain all (r_1, r_2), whose optima favor the ON and OFF state, respectively.

B. Constraint (C1) permits ON-favoring input

The optimization of $\bar{\mathbb{I}}(X, Y) = \bar{\mathbb{I}}(c_1, c_2)$ on the rectangular domain $0 < c_1 \le r_1, 0 < c_2 \le r_2$ in the (c_1, c_2)-plane varies qualitatively, depending on the location of the corner (r_1, r_2). As depicted in Fig. 2, we distinguish three regions A, B and C, which are separated by the two nullclines $\partial_1\bar{\mathbb{I}} = 0$ and $\partial_2\bar{\mathbb{I}} = 0$. The following analysis relies on the conjecture that both nullclines do not intersect except in the origin. Then the three regions are characterized by the signs of the partial derivatives $[\mathrm{sgn}(\partial_1\bar{\mathbb{I}}), \mathrm{sgn}(\partial_2\bar{\mathbb{I}})]$, taking on the values $[1, -1], [1, 1], [-1, 1]$ on A, B, C, respectively. The maximum (c_1^*, c_2^*) satisfies $c_1^* = r_1, c_2^* < r_2$ in region A, $c_1^* = r_1, c_2^* = r_2$ in region B and $c_1^* < r_1, c_2^* = r_2$ in region C. It is hence located in B or its boundary in all cases. The ratio $\chi := c_1^*/c_2^*$ reflects whether the optimal input process $X(t)$ favors the ON state ($\chi > 1$) or the OFF state ($\chi < 1$). For large r_1, r_2, paragraph I-B implies that the ratio χ approaches $1/(e-1)$. The asymmetry of the region B with respect to reflection at the bisection line causes a smaller region I favoring the ON state and a larger region II favoring the OFF state. If we assume a homogeneous constraint (C1) $\max\{c_1, c_2\} \le r_0$, closely related to [21], the bisection line transits from region B to region C, upon increasing r_0. This constraint thus implies a phase transition from symmetric ($\chi = 1$) to asymmetric ($\chi < 1$) allocation of the ON and the OFF state. An analogous transit behavior for the minimal sojourn time constraint has been reported in [21]. Fig. 3 shows the phase plane associated with the MI, i.e., when T is finite, for comparison with the results obtained for $\bar{\mathbb{I}}(X, Y)$.

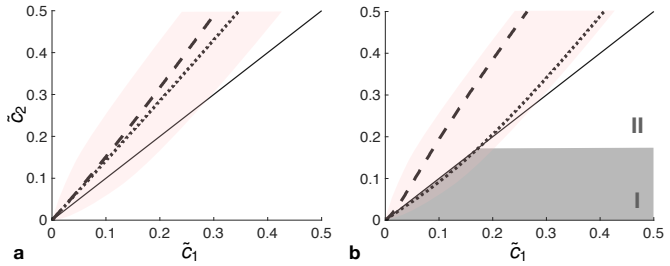


Fig. 3. Phase planes for finite T. **a** $T = 1$ **b** $T = 5$. Dotted and dashed lines indicate $\partial_1 \mathbb{I} = 0$ and $\partial_2 \mathbb{I} = 0$, respectively, and were obtained from numerically evaluating the integral in theorem III.1 on a grid with mesh 0.001. The red shaded area indicates region B of $\bar{\mathbb{I}}$, see Fig. 2, i.e., the case $T \to \infty$.

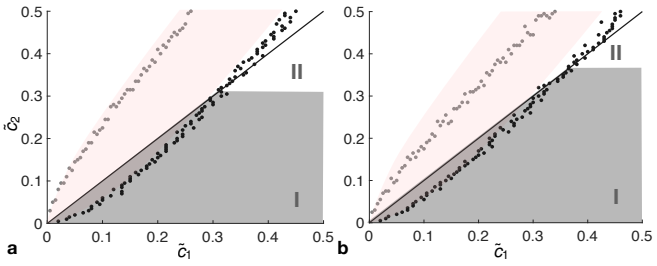


Fig. 4. Phase planes with leakage. **a** $x_1 = 0.01, x_2 = 1$ **b** $x_1 = 0.1, x_2 = 1$. Black and gray marks indicate the nullclines $\partial_1 \bar{\mathbb{I}} = 0$ and $\partial_2 \bar{\mathbb{I}} = 0$, respectively, and were obtained from Monte Carlo simulations with sample size $2 \cdot 10^6$. The red shaded area indicates region B of the case $x_1 = 0$.

C. Leakage does not alter the qualitative behavior

For a channel with leakage ($x_1 > 0$) the analogous evolution equation (4) reads

$$\frac{\partial}{\partial t} p(t,z) = -\frac{\partial}{\partial z}\{A(z-x_1)p(t,z)\} - c_3 z p(t,z) + c_3 f_-(z) p(t, f_-(z))\, \mathbb{1}(f_-(z) > \tilde{\omega}), \tilde{\omega} < z < x_2,$$

where $\tilde{\omega} := x_1 + \omega$ and $f_-(z) = \frac{x_1 x_2}{x_1 + x_2 - z}$ is the value of $Z(t_i-)$ that jumps to $Z(t_i+) = z$. The delay term $p(t, f_-(z))$ in the z-component turns it into an equation difficult to solve compared to (4). It is yet unclear, whether the asymptotic density $\pi(z)$ can be solved for, not to mention the time-evolving probability distribution. The first choice of technique for $\pi(z)$, method of steps [36], failed here, because the boundary value $\pi(f_-^{-1}(\tilde{\omega}))$ of the first interval $(\tilde{\omega}, f_-^{-1}(\tilde{\omega})]$ is yet unknown. Furthermore the successive intervals $(f_-^{-i}(\tilde{\omega}), f_-^{-(i+1)}(\tilde{\omega})], i \in \mathbb{N}_0$, where $f_-^0(\tilde{\omega}) := \tilde{\omega}, f_-^{-(i+1)} := f_-^{-1} \circ f_-^{-i}$, accumulate, because the sequence $f_-^{-i}(\tilde{\omega})_i$ monotonically approaches x_2.

Plots in Fig. 4 show results obtained from stochastic simulation of $Z(t)$ with sample size $2 \cdot 10^6$ and Monte Carlo evaluation of the mean in (1). While the qualitative behavior is not altered, leakage augments the asymptotic ratio from $\chi = 1/(e-1)$ (for $x_1 = 0$) to $\chi = 1$ (for $x_1 = 1$) if $x_2 = 1$ is fixed, according to paragraph I-B. Increasing leakage thus bends region B towards the bisection line and enlarges the ON-favoring region I.

D. Constraint (C2) enforces asymmetric allocation

Independent of the input states x_1, x_2, the autocorrelation time of X is $(c_1 + c_2)^{-1}$. The optimum of $\bar{\mathbb{I}}$ constrained to the triangular area (C2) $c_1 + c_2 \leq r_0$ is achieved on the diagonal boundary. The condition $\partial_1 \bar{\mathbb{I}} - \partial_2 \bar{\mathbb{I}} = 0$ determines the parametric curve of optimal rates in the c_1-c_2-plane. Hence it must lie in the region enclosed by the nullclines $\partial_1 \bar{\mathbb{I}} = 0$ and $\partial_2 \bar{\mathbb{I}} = 0$, i.e., in region B of Fig. 2. We observe strictly OFF-favoring, asymmetric, optimal allocations. For $c_1, c_2 \to 0$ symmetric allocation becomes asymptotically optimal for large minimal autocorrelation times.

E. Constraint (C3) allows for local optima

The quantity $\mathbb{E}[\mathbb{E}[\sigma_{X(t)}|X(t)]] = c_1^{-1} + c_2^{-1} - 2/(c_1 + c_2)$ is the expectation of the average sojourn times of the states x_1, x_2 taking into account stationarity of $X(t)$.

The constraint (C3) allows one rate to be infinite given the other is less than r_0. Thus its relevance seems to be questionable at first glance. Combination with other constraints that strictly determine the rates to be finite, like (C1) and (C2), legitimate (C3). Nevertheless we examined (C3) alone. The constraint defines a family of level sets $\mathbb{E}[\mathbb{E}[\sigma_{X(t)}|X(t)]] = r_0^{-1}$ in the (c_1, c_2)-plane, parametrized by r_0. The level set for each r_0 is a smooth curve, symmetric with respect to the bisection line. Regardless of r_0, the maximum of $\bar{\mathbb{I}}$ on each level set is assumed in the OFF-favoring region, i.e., above the bisection line. As r_0 decreases, at value $r_0 \approx 0.044$, a local maximum of $\bar{\mathbb{I}}$ appears in the ON-favoring region and perpetuates for smaller r_0, resembling a saddle-node bifurcation. Consequently, for average intertransition times greater than approximately $22.7/c_3$ high information throughput can be achieved by an ON-favoring rate pair. Both maxima approach the symmetric allocation as r_0 tends to zero.

IV. Conclusion

We considered the Poisson channel with BMPs as input class. The method of using the hybrid generator for the evolution of the causal estimator allowed to express its distribution in closed form and represent the MI and information rate by Riemann integrals. The information surface was then analyzed for different constraints on sojourn times. The mathematical derivation heavily relied on the Markov assumption and on neglecting leakage. Advancing mathematical results on leaking, Semi-Markov and multi-state inputs remain open problems. Among general binary inputs, our result yields a lower bound on the capacity.

Optimizing the allocation of the ON and the OFF state under constraint (C1) can be intuitively explained as an interplay between different forces that maximize the efficiency and precision of signal transmission. On the one hand, a force, reducing average sojourn times is predominant in region B of Fig. 2. This force aims at increasing the amount of signals transmitted. On the other hand, forces that increase the sojourn time in the ON and OFF states are predominant in regions

A and C, respectively. A larger sojourn time in the ON state increases the likelihood of observing the ON state at the channel output. A larger sojourn time in the OFF state decreases the likelihood of misinterpreting the period between consecutive channel output pulses as an input OFF phase. The phase diagram in Fig. 2 explicitly quantifies how the ensemble of forces is balanced. Constraint (C3) admits an analogous driving force towards its local maximum.

Given the analyzed model's rather minimal nature it might not account for biophysical reality. Yet assuming that evolutionary strategies aim at achieving capacity [25] the model supplies the hypothesis that system parameters $\tilde{c}_1, \tilde{c}_2$ are located in or near the optimal region B [37]. The prediction made by this interpretation is yet to be verified by experimentalists.

REFERENCES

[1] J. E. Purvis and G. Lahav, "Encoding and decoding cellular information through signaling dynamics," *Cell*, vol. 152, no. 5, pp. 945–956, 2013.

[2] D. Friedrich, L. Friedel, A. Finzel, A. Herrmann, S. Preibisch, and A. Loewer, "Stochastic transcription in the p53-mediated response to DNA damage is modulated by burst frequency," *Molecular Systems Biology*, vol. 15, no. 12, 2019.

[3] J. Selimkhanov, B. Taylor, J. Yao, A. Pilko, J. Albeck, A. Hoffmann, L. Tsimring, and R. Wollman, "Accurate information transmission through dynamic biochemical signaling networks," *Science*, vol. 346, no. 6215, pp. 1370–1373, 2014.

[4] F. Tostevin and P. R. ten Wolde, "Mutual information between input and output trajectories of biochemical networks," *Phys. Rev. Lett.*, vol. 102, p. 218101, 2009.

[5] A. Mugler, A. M. Walczak, and C. H. Wiggins, "Spectral solutions to stochastic models of gene expression with bursts and regulation," *Phys. Rev. E*, vol. 80, p. 041921, 2009.

[6] R. Suderman, J. A. Bachman, A. Smith, P. K. Sorger, and E. J. Deeds, "Fundamental trade-offs between information flow in single cells and cellular populations," *Proceedings of the National Academy of Sciences*, vol. 114, no. 22, pp. 5755–5760, 2017.

[7] G. Tkačik, C. G. Callan, and W. Bialek, "Information flow and optimization in transcriptional regulation," *Proceedings of the National Academy of Sciences*, vol. 105, no. 34, pp. 12 265–12 270, 2008.

[8] I. Lestas, G. Vinnicombe, and J. Paulsson, "Fundamental limits on the suppression of molecular fluctuations," *Nature*, vol. 467, no. 7312, p. 174, 2010.

[9] Y. Nakahira, F. Xiao, V. Kostina, and J. C. Doyle, "Fundamental limits and achievable performance in biomolecular control," in *2018 Annual American Control Conference (ACC)*, 2018, pp. 2707–2714.

[10] L. Duso and C. Zechner, "Path mutual information for a class of biochemical reaction networks," in *2019 IEEE 58th Conference on Decision and Control (CDC)*, 2019, pp. 6610–6615.

[11] S. A. Pasha and V. Solo, "Computing the trajectory mutual information between a point process and an analog stochastic process," in *2012 Annual International Conference of the IEEE Engineering in Medicine and Biology Society*. IEEE, 2012, pp. 4603–4606.

[12] S. Shamai, "Capacity of a pulse amplitude modulated direct detection photon channel," *IEE Proceedings I - Communications, Speech and Vision*, vol. 137, no. 6, pp. 424–430, 1990.

[13] K. V. Parag, "On signalling and estimation limits for molecular birth-processes," *Journal of theoretical biology*, vol. 480, pp. 262–273, 2019.

[14] A. Raj, C. S. Peskin, D. Tranchina, D. Y. Vargas, and S. Tyagi, "Stochastic mRNA synthesis in mammalian cells," *PLoS Biology*, vol. 4, no. 10, p. e309, 2006.

[15] C. Zechner, M. Unger, S. Pelet, M. Peter, and H. Koeppl, "Scalable inference of heterogeneous reaction kinetics from pooled single-cell recordings," *Nature Methods*, vol. 11, no. 2, pp. 197–202, 2014.

[16] O. Macchi and B. Picinbono, "Estimation and detection of weak optical signals," *IEEE Transactions on Information Theory*, vol. 18, no. 5, pp. 562–573, 1972.

[17] Y. M. Kabanov, "The capacity of a channel of the Poisson type," *Theory of Probability & Its Applications*, vol. 23, no. 1, pp. 143–147, 1978.

[18] M. Davis, "Capacity and cutoff rate for Poisson-type channels," *IEEE Transactions on Information Theory*, vol. 26, no. 6, pp. 710–715, 1980.

[19] D. Snyder and C. Georghiades, "Design of coding and modulation for power-efficient use of a band-limited optical channel," *IEEE Transactions on Communications*, vol. 31, no. 4, pp. 560–565, 1983.

[20] S. Shamai and A. Lapidoth, "Bounds on the capacity of a spectrally constrained Poisson channel," *IEEE Transactions on Information Theory*, vol. 39, no. 1, pp. 19–29, 1993.

[21] S. Shamai, "On the capacity of a direct-detection photon channel with intertransition-constrained binary input," *IEEE Transactions on Information Theory*, vol. 37, no. 6, pp. 1540–1550, 1991.

[22] L. Bintu, N. E. Buchler, H. G. Garcia, U. Gerland, T. Hwa, J. Kondev, and R. Phillips, "Transcriptional regulation by the numbers: models," *Current Opinion in Genetics & Development*, vol. 15, no. 2, pp. 116–124, 2005.

[23] D. M. Suter, N. Molina, D. Gatfield, K. Schneider, U. Schibler, and F. Naef, "Mammalian genes are transcribed with widely different bursting kinetics," *Science*, vol. 332, no. 6028, pp. 472–474, 2011.

[24] L. A. Mirny, "Nucleosome-mediated cooperativity between transcription factors," *Proceedings of the National Academy of Sciences*, vol. 107, no. 52, pp. 22 534–22 539, 2010.

[25] G. Tkačik and A. M. Walczak, "Information transmission in genetic regulatory networks: a review," *Journal of Physics: Condensed Matter*, vol. 23, no. 15, p. 153102, 2011.

[26] W. Bialek and S. Setayeshgar, "Physical limits to biochemical signaling," *Proceedings of the National Academy of Sciences*, vol. 102, no. 29, pp. 10 040–10 045, 2005.

[27] K. H. Kim and H. M. Sauro, "Measuring retroactivity from noise in gene regulatory networks," *Biophysical Journal*, vol. 100, no. 5, pp. 1167–1177, 2011.

[28] R. S. Liptser and A. N. Shiryaev, "Statistics of random processes II: Applications, vol. 2," *Springer*, vol. 737, p. 738, 2001.

[29] D. L. Snyder and M. I. Miller, *Random point processes in time and space*, ser. Springer texts in Electrical Engineering. Springer-Verlag, 1991.

[30] M. H. Davis, "Piecewise-deterministic Markov processes: A general class of non-diffusion stochastic models," *Journal of the Royal Statistical Society: Series B (Methodological)*, vol. 46, no. 3, pp. 353–376, 1984.

[31] C. Gardiner, *Stochastic methods: a handbook for the natural and social sciences, 4th ed.* Springer-Verlag, 2009.

[32] D. Guo, S. Shamai, and S. Verdú, "Mutual information and conditional mean estimation in Poisson channels," *IEEE Transactions on Information Theory*, vol. 54, no. 5, pp. 1837–1849, 2008.

[33] L. C. Evans, *Partial differential equations*. American Mathematical Society, 1998.

[34] P. Appell, "Sur les séries hypergéométriques de deux variables et sur dés équations différentielles linéaires aux dérivés partielles." *Comptes Rendus*, vol. 90, pp. 296–299, 731–735, 1880.

[35] H. M. Srivastava and P. W. Karlsson, *Multiple Gaussian hypergeometric series*. Ellis Horwood, 1985.

[36] R. D. Driver, *Ordinary and delay differential equations*. Springer Science & Business Media, 2012, vol. 20.

[37] A. Pérez-Escudero, M. Rivera-Alba, and G. G. de Polavieja, "Structure of deviations from optimality in biological systems," *Proceedings of the National Academy of Sciences*, vol. 106, no. 48, pp. 20 544–20 549, 2009.